Nanobeam photonic bandedge lasers

Sejeong Kim,[1] Byeong-Hyeon Ahn,[1,*] Ju-Young Kim,[1] Kwang-Yong Jeong,[1] Ki Soo Kim,[2] and Yong-Hee Lee[1,3]

[1]*Department of Physics, Korea Advanced Institute of Science and Technology, Daejeon 305-701, Korea*
[2]*Convergence and Components & Materials Research Laboratory, Electronics and Telecommunications Research Institute, Daejeon 305-700, Korea*
[3]*Graduate School of Nanoscience and Technology (WCU), Korea Advanced Institute of Science and Technology, Daejeon 305-701, Korea*
[*]*seygene@kaist.ac.kr*

Abstract: We demonstrate one-dimensional nanobeam photonic bandedge lasers with *InGaAsP* quantum wells at room temperature from the lowest dielectric band of photonic crystal nanobeam waveguides. The incident optical power at threshold is 0.6 mW (effectively ~18 μW). To confirm the lasing from the dielectric bandedge, the polarization and the photoluminescent spectra are taken from nanobeams of varying lattice constants. The observed shift of the lasing wavelength agrees well with the computational prediction.

OCIS codes: (203.5298) Photonic crystals; (140.5960) Semiconductor lasers.

References and links

1. O. Painter, R. K. Lee, A. Scherer, A. Yariv, J. D. O'Brien, P. D. Dapkus, and I. Kim, "Two-dimensional photonic band-Gap defect mode laser," Science **284**(5421), 1819–1821 (1999).
2. H.-G. Park, S.-H. Kim, S.-H. Kwon, Y.-G. Ju, J.-K. Yang, J.-H. Baek, S.-B. Kim, and Y.-H. Lee, "Electrically driven single-cell photonic crystal laser," Science **305**(5689), 1444–1447 (2004).
3. M.-K. Kim, J.-Y. Kim, J.-H. Kang, B.-H. Ahn, and Y.-H. Lee, "On-demand photonic crystal resonators," Laser Photon. Rev. **5**(4), 479–495 (2011).
4. H. Altug, D. Englund, and J. Vŭcković, "Ultrafast photonic crystal nanocavity laser," Nat. Phys. **2**(7), 484–488 (2006).
5. M.-K. Seo, J.-H. Kang, M.-K. Kim, B.-H. Ahn, J.-Y. Kim, K.-Y. Jeong, H.-G. Park, and Y.-H. Lee, "Wavelength-scale photonic-crystal laser formed by electron-beam-induced nano-block deposition," Opt. Express **17**(8), 6790–6798 (2009).
6. A. J. Shields, "Semiconductor quantum light sources," Nat. Photonics **1**(4), 215–223 (2007).
7. W.-H. Chang, W.-Y. Chen, H.-S. Chang, T.-P. Hsieh, J.-I. Chyi, and T.-M. Hsu, "Efficient single-photon sources based on low-density quantum dots in photonic-crystal nanocavities," Phys. Rev. Lett. **96**(11), 117401 (2006).
8. C. Santori, D. Fattal, J. Vucković, G. S. Solomon, and Y. Yamamoto, "Indistinguishable photons from a single-photon device," Nature **419**(6907), 594–597 (2002).
9. T. Yoshie, A. Scherer, J. Hendrickson, G. Khitrova, H. M. Gibbs, G. Rupper, C. Ell, O. B. Shchekin, and D. G. Deppe, "Vacuum Rabi splitting with a single quantum dot in a photonic crystal nanocavity," Nature **432**(7014), 200–203 (2004).
10. K. Hennessy, A. Badolato, M. Winger, D. Gerace, M. Atatüre, S. Gulde, S. Fält, E. L. Hu, and A. Imamoğlu, "Quantum nature of a strongly coupled single quantum dot-cavity system," Nature **445**(7130), 896–899 (2007).
11. H.-Y. Ryu, S.-H. Kwon, Y.-J. Lee, Y.-H. Lee, and J.-S. Kim, "Very-low-threshold photonic band-edge lasers from free-standing triangular photonic crystal slabs," Appl. Phys. Lett. **80**(19), 3476 (2002).
12. C. Monat, C. Seassal, X. Letartre, P. Regreny, P. Rojo-Romeo, P. Viktorovitch, M. Le Vassor d'Yerville, D. Cassagne, J. P. Albert, E. Jalaguier, S. Pocas, and B. Aspar, "InP based 2-D photonic crystal on silicon: In-plane Bloch mode laser," Appl. Phys. Lett. **81**(27), 5102–5104 (2002).
13. S.-H. Kwon, H.-Y. Ryu, G.-H. Kim, Y.-H. Lee, and S.-B. Kim, "Photonic bandedge lasers in two-dimensional square-lattice photonic crystal slabs," Appl. Phys. Lett. **83**(19), 3870–3872 (2003).
14. J. Mouette, C. Seassal, X. Letartre, P. Rojo-Romeo, J. L. Leclercq, P. Regreny, P. Viktorovitch, E. Jalaguier, P. Perreau, and H. Moriceau, "Very low threshold vertical emitting laser operation in InP graphite photonic crystal slab on silicon," Electron. Lett. **39**(6), 526–528 (2003).
15. S.-H. Kwon, S.-H. Kim, S.-K. Kim, Y.-H. Lee, and S. B. Kim, "Small, low-loss heterogeneous photonic bandedge laser," Opt. Express **12**(22), 5356–5361 (2004).
16. M. Nomura, S. Iwamoto, A. Tandaechanurat, Y. Ota, N. Kumagai, and Y. Arakawa, "Photonic band-edge micro lasers with quantum dot gain," Opt. Express **17**(2), 640–648 (2009).
17. M. Notomi, E. Kuramochi, and H. Taniyama, "Ultrahigh-Q nanocavity with 1D photonic gap," Opt. Express **16**(15), 11095–11102 (2008).

#154009 - $15.00 USD Received 2 Sep 2011; revised 17 Oct 2011; accepted 28 Oct 2011; published 10 Nov 2011

18. P. B. Deotare, M. W. McCutcheon, I. W. Frank, M. Khan, and M. Lončar, "High quality factor photonic crystal nanobeam cavities," Appl. Phys. Lett. **94**(12), 121106 (2009).
19. E. Kuramochi, H. Taniyama, T. Tanabe, K. Kawasaki, Y.-G. Roh, and M. Notomi, "Ultrahigh-Q one-dimensional photonic crystal nanocavities with modulated mode-gap barriers on SiO2 claddings and on air claddings," Opt. Express **18**(15), 15859–15869 (2010).
20. M. W. McCutcheon, P. B. Deotare, Y. Zhang, and M. Lončar, "High-Q transverse-electric/transverse-magnetic photonic crystal nanobeam cavities," Appl. Phys. Lett. **98**(11), 111117 (2011).
21. R. Ohta, Y. Ota, M. Nomura, N. Kumagai, S. Ishida, S. Iwamoto, and Y. Arakawa, "Strong coupling between a photonic crystal nanobeam cavity and a single quantum dot," Appl. Phys. Lett. **98**(17), 173104 (2011).
22. M. Eichenfield, R. Camacho, J. Chan, K. J. Vahala, and O. Painter, "A picogram- and nanometre-scale photonic-crystal optomechanical cavity," Nature **459**(7246), 550–555 (2009).
23. A. H. Safavi-Naeini, T. P. M Alegre, J. Chan, M. Eichenfield, M. Winger, Q. Lin, J. T. Hill, D. E. Chang, and O. Painter, "Electromagnetically induced transparency and slow light with optomechanics," Nature **472**(7341), 69–73 (2011).
24. B.-H. Ahn, J.-H. Kang, M.-K. Kim, J.-H. Song, B. Min, K.-S. Kim, and Y.-H. Lee, "One-dimensional parabolic-beam photonic crystal laser," Opt. Express **18**(6), 5654–5660 (2010).
25. Y. Zhang, M. Khan, Y. Huang, J. H. Ryou, P. B. Deotare, R. Dupuis, and M. Lončar, "Photonic crystal nanobeam lasers," Appl. Phys. Lett. **97**(5), 051104 (2010).
26. Y. Halioua, A. Bazin, P. Monnier, T. J. Karle, G. Roelkens, I. Sagnes, R. Raj, and F. Raineri, "Hybrid III-V semiconductor/silicon nanolaser," Opt. Express **19**(10), 9221–9231 (2011).
27. Y. Gong, B. Ellis, G. Shambat, T. Sarmiento, J. S. Harris, and J. Vučković, "Nanobeam photonic crystal cavity quantum dot laser," Opt. Express **18**(9), 8781–8789 (2010).
28. S. Mandal, X. Serey, and D. Erickson, "Nanomanipulation using silicon photonic crystal resonators," Nano Lett. **10**(1), 99–104 (2010).
29. M. M. Murshidy, A. M. Adawi, P. W. Fry, and D. G. Lidzey, "A one-dimensional photonic-crystal nanocavity incorporating a fluorescent molecular dye," Appl. Phys. Lett. **97**(15), 153303 (2010).
30. E. Kuramochi, H. Taniyama, T. Tanabe, K. Kawasaki, Y.-G. Roh, and M. Notomi, "Ultrahigh-Q one-dimensional photonic crystal nanocavities with modulated mode-gap barriers on SiO2 claddings and on air claddings," Opt. Express **18**(15), 15859–15869 (2010).
31. T. Baba and D. Sano, "Low-threshold lasing and Purcell effect in microdisk lasers at room temperature," IEEE J. Sel. Top. Quant. **9**(5), 1340–1346 (2003).

1. Introduction

Photonic Crystals (PhCs) provide versatile wavelength-scale optical platforms for photon control [1–16]. Small mode volume and high quality (Q) factor of a PhC cavity allow one to study low threshold lasers [1–5], single photon sources [6–8], and cavity quantum electrodynamics (QED) [9, 10] in semiconductor material systems. Over the last decade, many research groups have reported various forms of photonic crystal lasers. PhC lasers without a cavity or defects were also demonstrated by several groups [11–16]. This type of PhC laser takes advantages of the very low group velocity near the photonic band edge. So far, numerous PhC bandedge lasers have been demonstrated from two-dimensional (2-D) PhC structures [11–16]. The feedback mechanism is based on the periodic modulation of the entire structure. To reach lasing threshold, relatively large periodic structures were commonly required. In contrast, utilizing free-standing semiconductor PhC structures of high index contrast, 2-D photonic bandedge lasers having much smaller footprint were also realized [13].

Recently, one-dimensional (1-D) PhC structure was proposed by Notomi *et al.* [17]. Using this nano-ladder configuration, very small 1-D nanocavities having Qs of several hundreds of thousands were demonstrated [18–20] and cavity QED effects were successfully observed [21]. Very small mass of the nano-ladder enabled opto-mechanical studies [22, 23]. Low-threshold nanobeam lasers were also realized not only in the air but also in the water and glass backgrounds [24–27]. In these examples, photons are confined tightly in a small region near the cavity and the high electric field of the resonator can be used for optical trapping experiments [28, 29]. However, for certain bio-sensing applications, reasonable spatial overlap between the electric field and the object of interest is required. In the case of the defect mode laser, the point-like mode volume implies a very small interaction space. The fact that the object of interest should be in the close vicinity of the cavity limits the chance of particle trapping. In comparison, the 1-D photonic bandedge lasing covers the length of the nanobeam and this distributed electric field is expected to enhance the probability of particle trapping. In addition, one can take advantage of the freedom of position-independent pumping which is inherent to the 1-D translational symmetry of the nanobeam structure.

#154009 - $15.00 USD Received 2 Sep 2011; revised 17 Oct 2011; accepted 28 Oct 2011; published 10 Nov 2011

Here we report the 1-D nanobeam photonic bandedge laser having a distributed electric field profile. Typical Q-factors of 1-D nanobeam photonic bandedge are several tens of thousands. The small device volume leads to lasing at low threshold.

2. Design and computation

The 1-D photonic crystal nanobeam structure schematically described in Fig. 1(a) consists of an array of uniformly-sized periodic cylindrical air holes in a dielectric waveguide suspended in air. Typical dispersion characteristics are summarized in Fig. 1(b) where slab thickness, beam width, and air hole radius to be 0.8a, 1.5a, and 0.35a, where a is a lattice constant of periodic air holes. Note that only one wave vector is required to understand the behaviors of this waveguide. The lower three bands are described in the figure with electric field (E_y) distribution. The electromagnetic energy of the lowest band (red line) is localized in the dielectric region. This band is called dielectric band. On the other hand, the electromagnetic energy of the upper two bands is distributed near the air holes as shown in Fig. 1(b) (air bands). All bands are gradually flattened, when k_x approaches to 0.5. The group velocity becomes almost zero near the band edge (k_x = 0.5). This allows photons to stay longer inside the structure and to interact more with the gain medium.

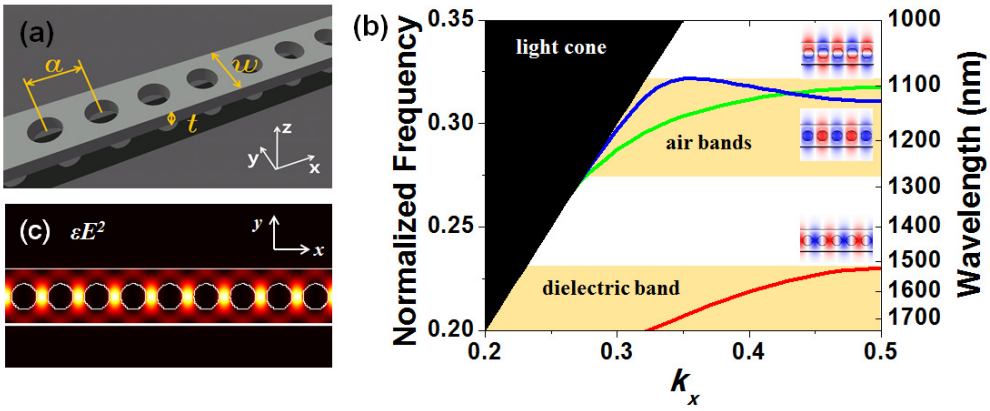

Fig. 1. (a) Schematics of 1-D periodic structure of nanobeam. (b) Dispersion characteristics of the structure. t = 0.8a, w = 1.5a, r = 0.35a. (c) Electric energy distribution of the dielectric band.

In this work, we focus on the dielectric band because it encourages strong interaction between photons and the dielectric gain medium. Photon distribution of the dielectric band is shown in Fig. 1(c). Typical Q factors of nanobeam bandedge modes are around several tens of thousands, larger than that of the 2-D counterpart [11, 13]. Figure 2 describes the effect of nanobeam length and nanobeam width on the Q factor. In Fig. 2(a), the Q factor increases monotonically with nanobeam length as expected. On the other hand, the effect of the nanobeam width is somewhat complicated. For a 60a-long nanobeam, the Q factor shows a maximum when the nanobeam width is about one lattice constant a as shown in Fig. 2(b). If one increases the nanobeam width while the air hole diameter is held fixed, the effective index contrast between the air hole and the dielectric regions becomes smaller, resulting in the higher group velocity and the lower Q factor. In contrast, when the width becomes thinner than the optimum value, the evanescent tail of the guided mode penetrates more deeply into the air and the resultant scattering losses at two ends of the finite-length nanobeam structure become more significant. However, it is encouraging to observe that the Q factor is over ten thousand for a 60a-long nanobeam of various beam widths (Fig. 2(b)), which turns out to be good enough for bandedge lasing. Lateral light confinement is achieved by the total internal reflection effect in y- and z- directions. For microfluidic applications, the nanobeam structure is placed in water where the low index contrast results in increased optical losses. It is worth

#154009 - $15.00 USD Received 2 Sep 2011; revised 17 Oct 2011; accepted 28 Oct 2011; published 10 Nov 2011

emphasizing that in the nanobeam structure one can always find 1-D photonic band gaps and, therefore, high-Q nanobeam structures can still be realized rather comfortably [30].

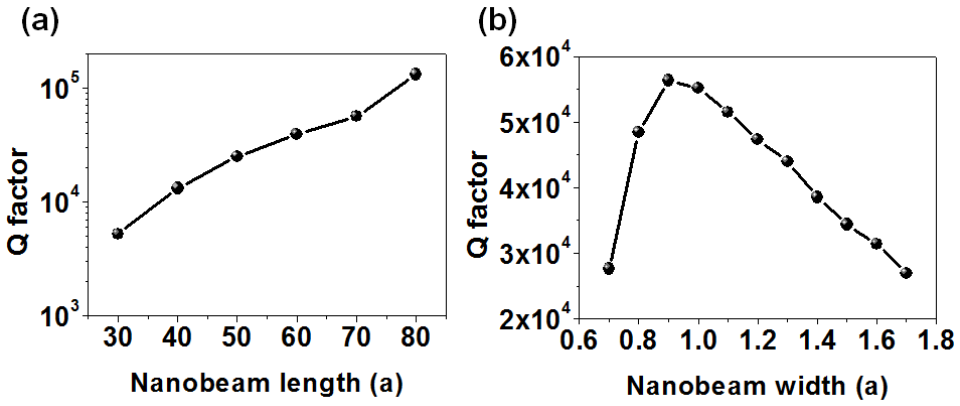

Fig. 2. (a) Q factor of nanobeam bandedge mode as a function of length. The radius of air holes and the nanobeam width are fixed to 0.35*a* and 1.5*a*. (b) Q factor as a function of nanobeam width. The radius of air holes and the nanobeam length are fixed to 0.35*a* and 60*a*, respectively.

3. Fabrication and measurement

1-D nanobeam structures are fabricated by electron beam lithography and Cl_2-assisted *Ar*-beam etching. The sacrificial *InP* layer was removed using $HCl{:}H_2O$ (4:1) solution to make free-standing nanobeams [15]. The nanobeam has three *InGaAsP* quantum wells having photoluminescence near 1.5 *μm*. Figure 3 shows scanning electron microscope (SEM) images of a fabricated sample: lattice constant, thickness, the radius of air holes, and beam width are 365 *nm*, 280 *nm*, 0.39*a*, and 1.55*a*, respectively.

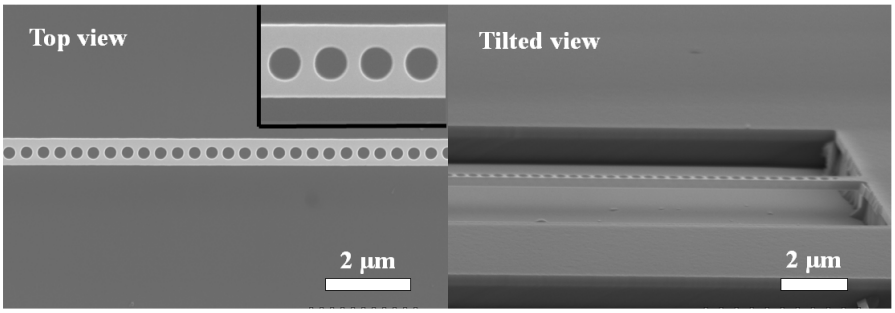

Fig. 3. SEM images of the fabricated sample. a = 365 *nm*, r = 0.39a, w = 1.55a.

A 980-*nm* laser diode was used for pumping. Pulse width was 10 *ns* and duty cycle was fixed to 1% to avoid thermal heating effects. The pumping beam was focused by a x20 microscope objective lens having numerical aperture (NA) of 0.45. Light emitted from the fabricated 1-D nanobeam was collected by the same objective lens and delivered to an IR camera combined with a monochromator of 1 *nm* resolution. The full-width at half-maximum of the pump spot was ~6 *μm*. In Fig. 4(a), lasing threshold is observed at pump power of ~0.6 *mW* at room temperature. This number is the incident optical power before the objective lens and the corresponding absorbed power by the slab is ~18 *μW* [31]. The output field is y-polarized as shown in the inset of Fig. 4(b), as predicted from the dielectric band of the nanobeam [18]. When pumped above threshold, this nanobeam laser operates in a single mode at 1552 *nm*, as shown in Fig. 4(b). In the quantum-well based bandedge laser, only one mode can reach the lasing condition because of the homogeneity of the gain material [16].

#154009 - $15.00 USD Received 2 Sep 2011; revised 17 Oct 2011; accepted 28 Oct 2011; published 10 Nov 2011

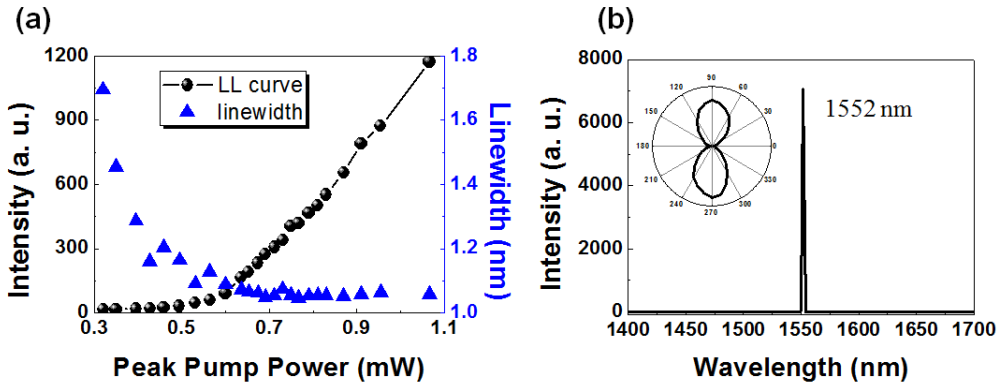

Fig. 4. (a) Light-in versus light-out curve and linewidth of the bandedge mode of the fabricated sample. Linewidth is limited by spectrometer resolution (~1*nm*) (b) Measured PL spectrum at the pumping power of 2.7 *mW* and polarization characteristics.

To confirm lasing at the dielectric bandedge, we fabricate and measure several patterns of different lattice constants. By varying the lattice constant from 310 *nm* to 430 *nm*, we achieved spectral tuning of the bands as shown in Fig. 5(a): the wavelength of the bandedge increases with lattice constant. Guide lines are the prediction by plane-wave expansion methods with the structure parameters specified in the caption of Fig. 5. Note that each mode agrees reasonably with the prediction within the fabrication error. In fact, the fabricated structures are generally not exactly equal to the computational designs because of the imperfections stemming from electron beam lithography and nanofabrication. The real fabricated structures have the air hole radius of $0.37a \pm 0.15a$ and the beam width of $1.57a \pm 0.034a$. In a sample with a large lattice constant, resonant PL peaks associated with air bandedge modes were also identified. In comparison, lasing action was not observed from the air bandedge mode because of its weak interaction between fields and gain materials. In Fig. 5(b), one can find both the dielectric- and the air-bandedge modes in single spectrum. Up to 400 *nm* lattice constant, nanobeam photonic bandedge lasers operate in a single mode, which can be advantageous for application point of view.

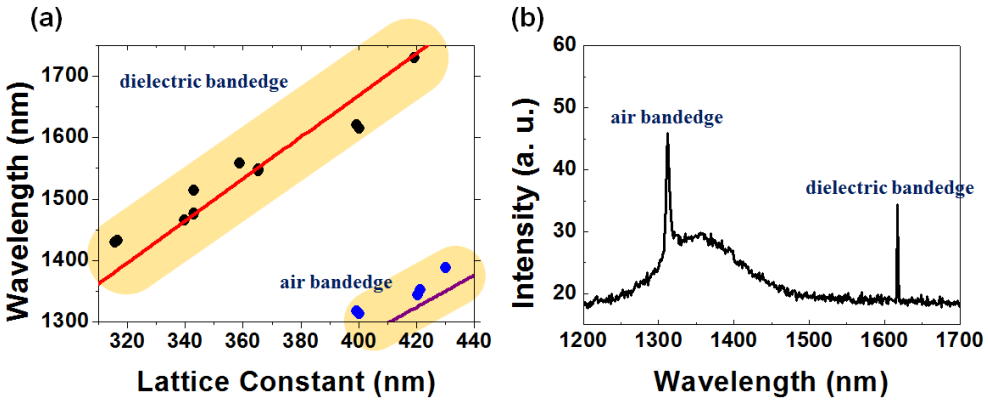

Fig. 5. (a) Variation of dielectric and air bandedges with lattice constant. Guide lines are computational results with $r = 0.37a$, $w = 1.5a$, and $t = 280$ *nm*. (b) PL spectrum of $a = 400$ *nm*. Two bandedges are observed simultaneously.

4. Summary

We investigated bandedge lasing from free-standing 1-D nanobeam structures. Low effective optical threshold of ~18 μW is achieved. Lasing at the dielectric bandedge was confirmed by

#154009 - $15.00 USD Received 2 Sep 2011; revised 17 Oct 2011; accepted 28 Oct 2011; published 10 Nov 2011

the structural tuning and polarization measurements. We believe that this type of bandedge laser, without cavity, is useful for bio-sensing applications [28, 29] and opto-mechanical applications [22, 23]. Also, their small physical size is a benefit for the photonic integrated circuits.

Acknowledgement

This research was supported by WCU (World Class University) program through KOSEF (Korea Science and Engineering Foundation) funded by the Ministry of Education, Science and Technology (grant number: R31-2010-000-10071-0), by the National Research Foundation of Korea funded by the Korea government (MEST) (grant number: 2009-0093863), and by Basic Science Research Program through the National Research Foundation of Korea funded by the Ministry of Education, Science and Technology (grant number: 2009-0087691). B.-H. Ahn is supported by National Junior Research Fellowship which National Research Foundation of Korea conducts from 2010.

#154009 - $15.00 USD Received 2 Sep 2011; revised 17 Oct 2011; accepted 28 Oct 2011; published 10 Nov 2011